Available online at www.sciencedirect.com

SciVerse ScienceDirect

Procedia Engineering 00 (2017) 000–000

Procedia Engineering

www.elsevier.com/locate/procedia

X International Conference on Structural Dynamics, EURODYN 2017

Active Modal Control of Rain-Wind Induced Vibration of Stay Cables

Niels Holm Krarup[a], Zili Zhang[a,*], Poul Henning Kirkegaard[a]

[a]*Department of Engineering, Aarhus University, 8000 Aarhus, Denmark*

Abstract

Rain-wind induced vibrations have been observed on numerous cable-stayed bridges around the world, which has resulted in an urgent need to gain further understanding of the phenomenon and to develop efficient means of mitigating the large-amplitude vibrations. It is believed that this aeroelastic instability problem is due to the formation and oscillation of a water rivulet on the upper cable surface, which changes the cable aerodynamics and absorbs energy into the system. In this paper, an analytical study of the phenomenon is conducted by formulating a finite element model for the cable and the upper rivulet with non-linear coupling effect. Linearization of the equations of motion of the cable-rivulet system is next carried out, based on which active vibration controller can be designed. Pole allocation control method has been employed for mitigating RWIV in the present study, which is able to add sufficient damping to several excited modes. The active controller is designed such that the closed-loop poles are allocated on the left half of the complex plane of eigenvalues. The controller gains obtained from the equivalent linear system are then applied to the original non-linear cable-rivulet system. Simulation results show that the proposed active modal controller performs much better in suppressing RWIV than an optimally tuned linear viscous damper.

Peer-review under responsibility of the organizing committee of EURODYN 2017.

Keywords: Stay cable, rain-wind induced vibration, FE model, active vibration control, pole allocation method

1. Introduction

Ever since the phenomenon originally described in late 1980s [1], rain-wind induced vibration (RWIV) of stay cables in cable-stayed bridges has been a much debated research topic and is presently a great concern to wind engineering communities. RWIV is characterized by large-amplitude vibrations occurring under the combined action of moderate wind and moderate to heavy rain. It is believed that this aeroelastic instability problem is due to the formation and oscillation of a water rivulet on the upper cable surface, which changes the cable aerodynamics and absorbs energy into the system. RWIV is similar to galloping vibration of bars with an asymmetric cross-section, but the essential difference is that the cable vibration will induce local oscillations of the rivulets from their equilibrium position, resulting in a highly coupled aeroelastic system. This phenomenon has been investigated through field measurement [1], wind tunnel tests [1] and theoretical analyses [2]. In wind tunnel tests, the rivulet on the cable

* Corresponding author. Tel.: +4593508334
E-mail address: zili_zhang@eng.au.dk

Peer-review under responsibility of the organizing committee of EURODYN 2017.

section model (rigid) is mimicked by spraying water onto the cable surface or by sticking artificial rivulet model, from which the vibration characteristics and the aerodynamic coefficients can be obtained. Theoretical studies have been mainly based on 2D rigid sectional cable model and quasi-steady assumptions, even though unsteady aerodynamic model has also been proposed [3]. Although it is widely believed that the upper rivulet and its motion play important roles in RWIV, further studies are still needed for a deeper and thorough understanding of the complex phenomenon.

Traditionally, RWIV has been mitigated using both aerodynamic and mechanical control strategies. Aerodynamic countermeasures include the use of a protuberated polyethylene-lapped cables as well as wounding metal wire helicoidally around the cables [4]. These methods are far less well-understood and are mostly based on experience from experiments. On the other hand, one useful mechanical approach is the installation of cable cross-ties [5], which effectively increases damping in the cable at the cost of violating the bridge aesthetics. Linear viscous dampers (oil dampers) attached close to the lower support point [6] are widely used for cable vibration control in practice. This kind of passive damper is usually optimally tuned to a single mode and does not supply sufficient damping to other modes, which may be a potential problem for RWIV where several modes can be excited in certain circumstances.

In this paper, the response of a single stay cable excited by RWIV is simulated using a finite element (FE) model. A model describing the interaction between the vibrating cable and the oscillating upper rivulet with an overcritical nonlinear damping mechanism is combined with the FE model, to obtain a full set of nonlinear equations of motion (EOM) of the cable-rivulet system. The established model is able to predict some key characteristics of RWIV. Next, a pole allocation type of active modal controller is proposed for mitigating RWIV, which is able to add sufficient damping to several excited modes. To facilitate the design of the active controller, an equivalent linearization is carried out on the nonlinear EOM of the cable-rivulet system. Based on the equivalent linear system, the active controller is designed such that the closed-loop poles are placed on the left half of the complex plane of the eigenvalues (positive modal damping). The controller gains obtained from the equivalent linear system are then applied to the original nonlinear cable-rivulet system. Performance of the active modal controller is compared with that of an optimally tuned linear viscous damper (oil damper), and significant improvement in suppressing RWIV has been achieved.

2. FE model of the cable-rivulet system

A structural dynamic model for the cable-rivulet system is established. The cable is modelled by a FE model consisting of N standard cable elements, and an existing nonlinear model for the oscillating rivulet has been extended to be combined into the FE cable model. Quasi-steady assumption is employed to calculate the aerodynamic loads.

2.1. FE modelling of the cable

Fig. 1a shows a cable with a length L and mass per unit length μ, subjected to a tension force T. The cable displacements are described in a planar (x, y)- coordinate system, with x- axis placed along the cable. N numbers of finite elements are used in the FE model with $N-1$ numbers of non-constrained nodes as shown in Fig. 1a. Based on Galerkin variational method with linear element shape functions, element mass and stiffness matrices are established, from which the equations of motion of the cable can be formulated as:

$$\mathbf{M}_0\ddot{\mathbf{u}}(t) + \mathbf{C}_0\dot{\mathbf{u}}(t) + \mathbf{K}_0\mathbf{u}(t) = \mathbf{P}_0(t) \tag{1}$$

where $\mathbf{M}_0$ and $\mathbf{K}_0$ are the $(N-1)\times(N-1)$ dimensional consistent mass and stiffness matrices, respectively. $\mathbf{C}_0$ is the structural damping matrix obtained using Rayleigh damping model. $\mathbf{u}(t)$ is an $(N-1)$- dimensional vector containing the nodal displacements, and $\mathbf{P}_0(t)$ is an $(N-1)$-vector representing the aerodynamic load acting at the nodes.

2.2. Modeling of the rivulet motion

The rivulet model proposed in [7] is adopted and extended in this paper. The motion of the rivulet is modeled as a 1-DOF oscillator vibrating in the circumferential direction around its equilibrium position θ_0, with the cable vibration as the excitation. With the sign definitions in Fig. 1b, the equation of motion of the rivulet can be expressed as:

$$\ddot{\theta} + 2\zeta_r\omega_r|\dot{\theta}|^{\alpha_r}\dot{\theta} + \omega_r^2\theta = \frac{\ddot{u}\sin(\theta_0+\theta)}{R} \tag{2}$$

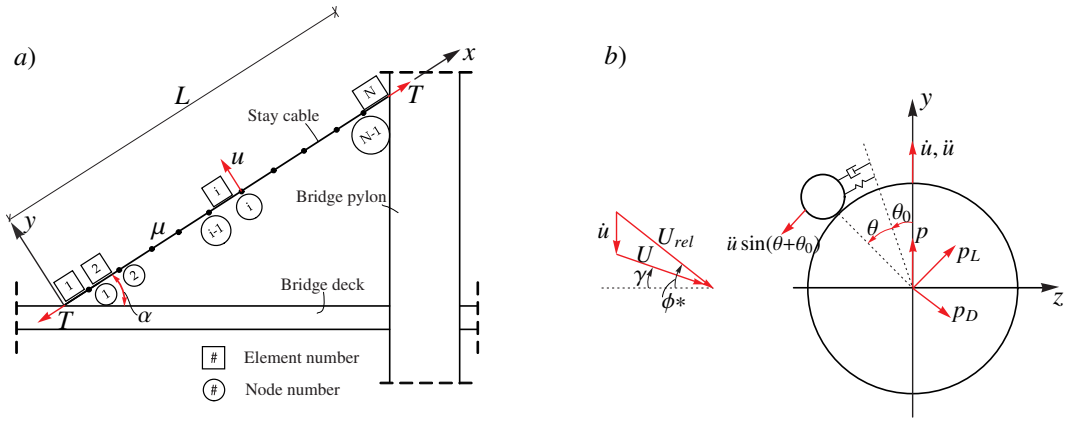

Fig. 1: FE model of the cable-rivulet system. a) Definition of coordinate system and numbering of nodes and elements in FE model. b) SDOF oscillator model of the rivulet motion and definition of aerodynamic loadings.

where $\theta(t)$ is the degree of freedom describing the rivulet motion (angle) relative to the equilibrium angle θ_0. R is the cable radius, ζ_r is the damping ratio of the rivulet and α_r is a damping exponent which determines the damping law describing all damping forces (aerodynamic damping and friction) acting on the rivulet. It should be noted that $\alpha_r = 0$ and $\alpha_r = 1$ corresponds to linear viscous damping and fluid damping models, respectively. ω_r is the angular eigenfrequency of the oscillating rivulet, with the restoring force originating from water surface tension. Based on test results, it is suggested that ω_r simply chosen as the fundamental eigenfrequency ω_1 of the cable [1]. $\ddot{u}(x,t)$ is the acceleration of the cable in the y- direction. Assuming that the rivulet motion $\theta(t)$ is constant within each cable element and that the cable acceleration at the mid-point of each cable element is the average cable acceleration of the adjacent nodes, the rivulet model can be extended to an N-DOF model expressed in the following matrix form:

$$\ddot{\boldsymbol{\theta}}(t) + \mathbf{C}_r(\dot{\boldsymbol{\theta}})\,\dot{\boldsymbol{\theta}}(t) + \mathbf{K}_r\,\boldsymbol{\theta}(t) - \mathbf{M}_r(\boldsymbol{\theta})\,\ddot{\mathbf{u}}(t) = \mathbf{0} \tag{3}$$

where

$$\underset{N\times N}{\mathbf{K}_r} = \omega_r^2 \begin{bmatrix} 1 & 0 & \dots & 0 \\ 0 & 1 & \dots & 0 \\ \vdots & \vdots & \ddots & 0 \\ 0 & 0 & \dots & 1 \end{bmatrix}, \quad \underset{N\times N}{\mathbf{C}_r(\boldsymbol{\theta})} = 2\zeta_r\omega_r \begin{bmatrix} |\dot{\theta}_1|^{\alpha_r} & 0 & \dots & 0 \\ 0 & |\dot{\theta}_2|^{\alpha_r} & \dots & 0 \\ \vdots & \vdots & \ddots & \vdots \\ 0 & 0 & \dots & |\dot{\theta}_N|^{\alpha_r} \end{bmatrix}, \quad \underset{N\times(N-1)}{\mathbf{M}_r(\boldsymbol{\theta})} = \frac{1}{2R} \begin{bmatrix} \sin(\theta_1+\theta_0)\cdot\mathbf{p}_1^T \\ \sin(\theta_2+\theta_0)\cdot(\mathbf{p}_1^T+\mathbf{p}_2^T) \\ \vdots \\ \sin(\theta_{N-1}+\theta_0)\cdot(\mathbf{p}_{N-2}^T+\mathbf{p}_{N-1}^T) \\ \sin(\theta_N+\theta_0)\cdot\mathbf{p}_{N-1}^T \end{bmatrix} \tag{4}$$

$\boldsymbol{\theta}(t) = [\theta_1(t), \theta_2(t), \cdots, \theta_N(t)]^T$ is the degrees of freedom vector of the rivulet movements. The position vector $\mathbf{p}_i$, $i = 1, 2, \cdots, N-1$, is an $N-1$ dimensional column vector having 1 at the i'th entry and 0 at all others. Eq. (3) represents a non-linear system due to the non-linearities introduced from the damping of the rivulet and the inertia term related to the component of the cable acceleration in the circumferential direction.

2.3. Aerodynamic load

Quasi-steady assumption is used for calculating the aerodynamic loads acting on the cable. The load per unit length in y- direction $p(x,t)$, which contributes to the load vector $\mathbf{P}_0(t)$, can thus be written as (Fig. 1b):

$$p(x,t) = \rho R U_{rel}^2 [C_l(\phi)\cos(\phi^*) - C_d(\phi)\sin(\phi^*)] \tag{5}$$

where ρ is mass density of air. $C_l(\phi)$ and $C_d(\phi)$ are the lift and drag coefficients. The relative velocity between the wind and the cable U_{rel}, the inflow angle ϕ^*, and the effective angle of attack ϕ are expressed as:

$$\begin{cases} U_{rel}^2 = (U\cos\gamma)^2 + (U\sin\gamma + \dot{u})^2 \\ \phi^* = tan^{-1}(\frac{U\sin\gamma+\dot{u}}{U\cos\gamma}) \\ \phi = \phi^* - \theta - \theta_0 \end{cases} \tag{6}$$

$\dot{u}$ represents the cable velocity at the mid-point of each element. ϕ^* and ϕ are denoted in Fig. 1b. U and γ are the component of the mean wind perpendicular to the cable axis and its angle, respectively, which can be expressed as:

$$U = U_0 \sqrt{\cos^2\beta + \sin^2\alpha \sin^2\beta}\,, \quad \gamma = \epsilon \sin^{-1}\left(\sin\beta \sin\alpha \Big/ \sqrt{\cos^2\beta + \sin^2\alpha \sin^2\beta}\right) \tag{7}$$

where U_0 is the mean wind speed far upstream, α is the cable inclination and β is the yaw angle of the mean wind with respect to the cable plane. ϵ is an influence factor ($0 \le \epsilon \le 1$) suggested in [7].

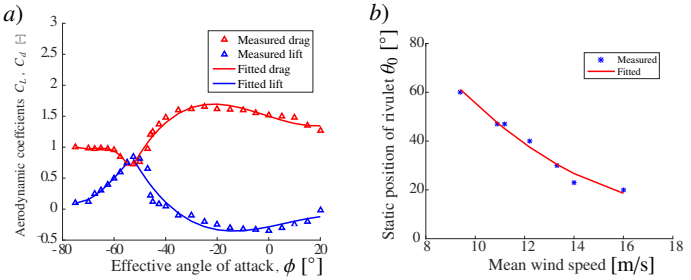

Fig. 2: Parameters related to aerodynamic loads. a) Lift and drag coefficients as a function of the effective angle of attack. b) Equilibrium angle θ_0 as a function of mean wind speed.

Fig. 2a shows the dependence of lift and drag coefficients as a function of the effective angle of attack ϕ, obtained from wind tunnel test [4]. The equilibrium position of the rivulet denoted by θ_0 is a decreasing function of the mean wind speed, as shown by the experimental results in Fig. 2b [1]. This makes sense because the rivulet is pushed further up on the cable surface with increased wind speed.

3. Active modal control of RWIV

The non-linear EOMs of the cable-rivulet system are linearized, based on which active controller are designed. The obtained controller gains are then applied to the original non-linear equations for feedback vibration control.

3.1. Linearization of EOM

The aerodynamic load per unit length $p(x,t)$ in Eq. (5) is linearized using Taylor expansion, and the load vector $\mathbf{P}_0(t)$ in Eq. (1) can then be expressed as:

$$\mathbf{P}_0(t) = \bar{\mathbf{P}}_0 - \mathbf{C}_a\,\dot{\mathbf{u}}(t) - \mathbf{K}_a\,\boldsymbol{\theta}(t) \tag{8}$$

where $\mathbf{C}_a$ and $\mathbf{K}_a$ are the aerodynamic damping and stiffness matrices. $\bar{\mathbf{P}}_0$ is a constant load vector due to mean wind. The non-linear EOM of the rivulet in Eq. (3) are also linearized around its static equilibrium, with stochastic linearization technique [8] applied to the damping matrix. The linearized format of Eqs. (1) and (3) becomes:

$$\begin{cases} \mathbf{M}_0\,\ddot{\mathbf{u}}(t) + (\mathbf{C}_0 + \mathbf{C}_a)\,\dot{\mathbf{u}}(t) + \mathbf{K}_0\,\mathbf{u}(t) + \mathbf{K}_a\,\boldsymbol{\theta}(t) = \bar{\mathbf{P}}_0 \\ \ddot{\boldsymbol{\theta}}(t) + \bar{\mathbf{C}}_r\,\dot{\boldsymbol{\theta}}(t) + \mathbf{K}_\mathbf{r}\,\boldsymbol{\theta}(t) - \bar{\mathbf{M}}_r\,\ddot{\mathbf{u}}(t) = \mathbf{0} \end{cases} \tag{9}$$

which can be combined, leading to the following linearized EMO of the cable-rivulet system:

$$\mathbf{M}\,\ddot{\mathbf{w}}(t) + \mathbf{C}\,\dot{\mathbf{w}}(t) + \mathbf{K}\,\mathbf{w}(t) = \mathbf{P} \tag{10}$$

where $\mathbf{w}(t) = [\mathbf{u}(t)^T, \boldsymbol{\theta}(t)^T]^T$ is the $2N-1$ dimensional degrees of freedom vector.

3.2. Active modal controller design

Eq. (10) can be further reformulated into the linear state vector equation:

$$\frac{d}{dt}\mathbf{z} = \mathbf{A}\mathbf{z} + \mathbf{f} + \mathbf{b}_c f_c(t) \tag{11}$$

where $\mathbf{z}(t) = [\mathbf{w}(t)^T, \dot{\mathbf{w}}(t)^T]^T$ is the $4N-2$ dimensional state vector. $f_c(t)$ is the control force applied by the controller, i.e. an actuator installed close to the lower support point. In principle, different active control laws can be established based on the linear state vector equation, e.g. LRQ method. In the present paper, the pole allocation method is employed, with the advantage that the modal damping introduced to different modes can be quantified and manipulated by the designer. The idea is to prescribe the closed-loop poles of the closed-loop system (the cable-rivulet system with controller) associated with the modes to be controlled, and then compute the controller gains required to produce these poles [9]. Following the procedure in [9], the control force and the corresponding controller gains can be determined:

$$f_c(t) = -\sum_{j=1}^{2m_1} g_j \mathbf{\Psi}_j^T \mathbf{z}(t), \qquad g_j = -\frac{\prod_{k=1}^{2m_1}(\rho_k - \lambda_j)}{p_j \prod_{\substack{k=1 \\ k\neq j}}^{2m_1}(\lambda_k - \lambda_j)}, \quad j = 1, 2, ..., 2m_1 \tag{12}$$

where m_1 represents the number of modes to be controlled. g_j are the controller gains which are pair-wise complex conjugated. $\mathbf{\Psi}_j$ are the left eigenvectors (adjoint eigenvectors) of the open-loop system matrix $\mathbf{A}$ in Eq. (11). λ_j are the poles of the open-loop system. ρ_k are the prescribed closed-loop poles for the controlled modes, determined by the designer. The constants p_j can be determined from the right eigenvectors $\mathbf{\Phi}_j$ of matrix $\mathbf{A}$ [9]. It should be noted that the active modal controller assumes full state observation of $\mathbf{z}(t)$, and therefore an observer has to be designed.

4. Simulation results

Table 1: Cable and rivulet parameters used in the FE model

Parameters	L (m)	D (m)	T (N)	μ (kg/m)	ζ_s	α (°)	β (°)	ϵ	ζ_r	α_r
Value	150	0.140	1.147×10^6	51	0.005	45	45	0.4	10	1

The set of cable and rivulet parameters shown in Table 1 have been used in the simulation. It is observed that the cable without control exhibits large RWIVs under the wind speed ranging from 9 m/s to 11 m/s. The large amplitude vibrations are dominated by the fundamental cable mode, and therefore the modes to be controlled by the active controller is $m_1 = 1$ in the present case, although multi-mode control can be easily implemented. The performance of an optimal tuned (to the fundamental mode) linear viscous damper (oil damper) is also investigated, with the optimal damping coefficient determined from [6].

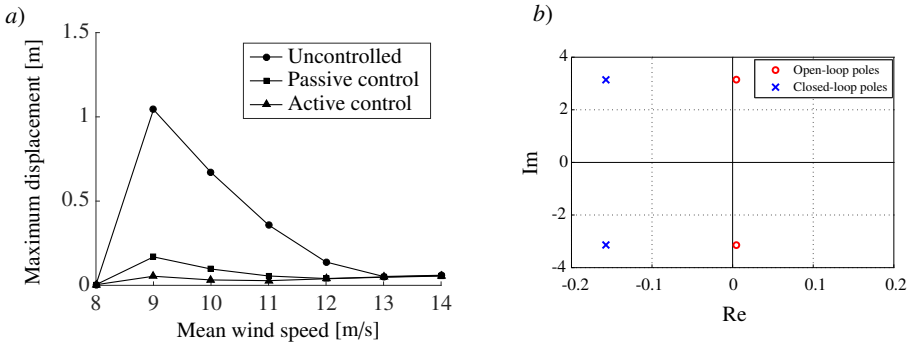

Fig. 3: Performance of the active modal controller. a) Peak cable response under different mean wind speeds with and without control. b) Open-loop poles and closed-loop poles of the 1st cable mode, U_0=9 m/s.

Fig. 3a shows the maximum displacement of the cable at mid point under different mean wind speeds, for cases without control, with optimal linear viscous damper and with active modal controller. It is shown that the largest response of the cable without control takes place at $U_0 = 9$ m/s. Both the optimal passive damper and the active controller effectively suppress the vibration amplitude. The proposed active modal controller performs better and almost completely eliminates cable vibrations. In the present case, the active modal controller is designed based on a desired damping ratio for the first cable mode of $\zeta = 0.5\%$. The resulting closed-loop poles of the first cable mode

are shown in Fig. 3b, together with the open-loop poles at $U_0 = 9$ m/s. It is clearly seen that the open-loop poles have positive real part, implying negative modal damping, which is the reason for large vibration amplitude shown in Fig. 3a. With the active controller, the closed-loop poles are placed on the left side of the complex plane. It should be noted that the prescribed closed-loop poles are only used for calculating the controller gains, based on which the active control force is applied to the original non-linear cable-rivulet system.

Fig. 4a shows the time-series of the cable displacement at mid point, for cases without control, with optimal linear viscous damper and with active modal controller. Without control, the cable vibration increases exponentially to around 1 m and then maintains this amplitude-restricted vibration due to the nonlinear interaction between the cable and the rivulet. Although the optimal passive damper effectively reduce the amplitude of vibrations, it is unable to eliminate vibrations entirely. On the other hand, the active modal controller appears to eliminate vibrations entirely after a certain period. As a result, the required active control force becomes almost zero as well after this period, as shown in Fig. 4b. Moreover, even from the beginning, the active control force is smaller than the passive damping force, making the active controller more competitive.

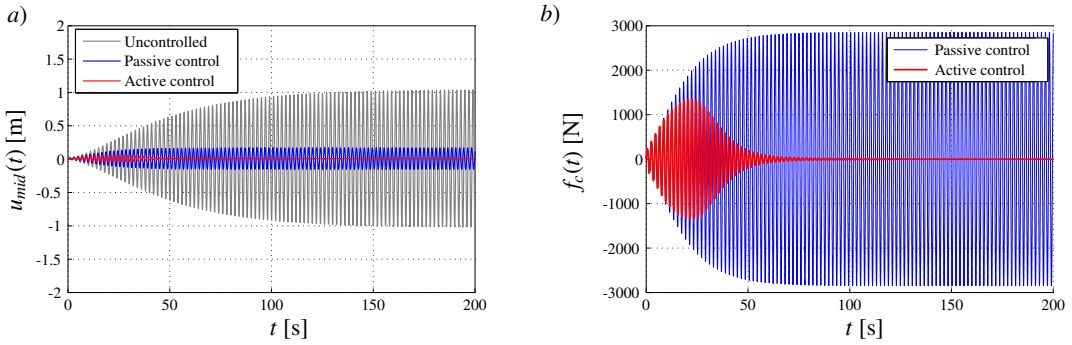

Fig. 4: Time-series of the cable responses and the control forces, U_0=9 m/s. a) Cable displacements at mid point. b) Control force.

5. Conclusions

A FE model for the stay cable with oscillating upper rivulet is established, which is able to predict key characteristics of RWIV. Next, a pole allocation type active modal controller is designed based on the linearized EOM of the non-linear cable-rivulet system. The advantage of the active modal controller is that sufficient damping can be introduced to several excited modes only by properly allocating the poles of the closed-loop system. Simulation results indicate that the proposed controller can efficiently suppress the RWIV, and significant improvement has been achieved comparing with an actively tuned linear viscous damper.

References

[1] Y. Hikami, N. Shiraishi, Rain-Wind Induced Vibration of Cables in Cable-Stayed Bridges, Journal of Wind Engineering and Industrial Aerodynamics. 29 (1988) 409-418.
[2] Y.L. Xu, L.Y. Wang, Analytical Study of Wind-Rain Induced Vibration: SDOF Model, Journal of Wind Engineering and Industrial Aerodynamics. 91 (2003) 27-40.
[3] M. Matsumoto, et al., Motion-effect of water rivulet on rain-wind induced vibration of inclined stay-cables, Journal of Wind Engineering and Industrial Aerodynamics. 91 (2003) 27-40.
[4] M. Gu, X. Du, Experimental investigation of rain-wind-induced vibration of cables in cable-stayed bridges and its mitigation, Journal of Wind Engineering and Industrial Aerodynamics. 93 (2005) 79-95.
[5] H. Yamaguchi, H.D. Nagahawatta, Damping effects of cable cross ties in cable-stayed bridge, Journal of Wind Engineering and Industrial Aerodynamics. 54-55 (1995) 35-43.
[6] S. Krenk, Vibrations of a Taut Cable With an External Damper, Journal of Applied Mechanics. 67 (2000) 772-776.
[7] L.Y. Wang, Y.L. Xu, Analytical Study of Wind-Rain Induced Vibration: 2DOF Model, Wind and Structures vol. 6. 4 (2003) 291-306.
[8] Y.L. Xu, B. Samali, K. C. S. Kwok, Control of Along-Wind Response of Structures by Mass and Liquid Dampers, Journal of Engineering Mechanics. 118 (1992), 20-39.
[9] L. Meirovitch, Dynamics and Control of Structures, John Wiley & Sons, 1990.